S0013-4651(99)03-102-X CCC: $7.00 © The Electrochemical Society, Inc.

Alternatives to Hydrogen Fluoride for Photoelectrochemical Etching of Silicon

M. M. Rieger,[a,*] J. C. Flake,[b,] and P. A. Kohl[b,*]**

[a]*Department of Chemical Engineering and Materials Science, University of Oklahoma, Norman, Oklahoma 73019, USA*
[b]*School of Chemical Engineering, Georgia Institute of Technology, Atlanta, Georgia 30332-0100, USA*

Photoelectrochemical etching of silicon in nonaqueous solutions without the use of free-fluoride or HF has been demonstrated. Silicon was electrochemically oxidized and dissolved using stable, fluoride containing salts in acetonitrile solutions. The current-voltage behavior of silicon in acetonitrile solutions containing tetrabutylammonium tetrafluoroborate or tetrabutylammonium hexafluorophosphate were similar. The voltammetry of silicon in solutions containing tetrabutylammonium trifluoromethylsulfonyl, potassium hexafluoroarsenate, or sodium hexafluoroantimonate showed large hysteresis indicating the presence of silicon oxide on the surface. Although the dissolution rate of silicon dioxide was negligible in the absence of free-fluoride or HF, the oxidation and dissolution of silicon could be maintained, even when thin oxides were formed. Photocurrent oscillations associated with the buildup and removal of oxides were observed when traces of water were present.
© 1999 The Electrochemical Society. S0013-4651(99)03-102-X. All rights reserved.

Manuscript submitted March 24, 1999; revised manuscript received July 7, 1999.

The photoelectrochemical etching of silicon in aqueous electrolytes involves the participation of water in the formation and dissolution of silicon oxides.[1,2] In the absence of free-fluoride or HF, the oxidized silicon is complexed by water, resulting in an oxide layer which electrically passivates the surface. The formation of higher quality (dense) oxides and lower-quality oxides has been studied in aqueous electrolytes as a function of current density, potential, and time.[3-6] In aqueous electrolytes at potentials above the critical current peak, electropolishing occurs where a steady-state condition of oxide formation and dissolution is established.

The electrochemical oxidation of silicon is initiated by valence band holes and results in tetravalent dissolution as SiF_6^{2-} when free-fluoride is present. The sustained etching of silicon is achieved when free-fluoride (or HF) is available to complex the oxidized silicon and/or dissolve the oxide. Ohmi *et al.* have identified HF_2^- as the dominant fluoride species most often responsible for silicon dioxide dissolution in aqueous solutions.[7] In a previous work, it was demonstrated that silicon may be electrochemically etched in nonaqueous electrolytes containing either anhydrous HF or tetrabutylammonium fluoroborate ($TBABF_4$).[8] It is important to note that the chemical and electrochemical behavior of these two fluoride sources (HF and $TBABF_4$) are quite different because of the stability of the fluoroborate complex and the absence of free fluoride. It is well known that SiO_2 is chemically stable and does not dissolve in aqueous or nonaqueous $TBABF_4$ solutions. Furthermore, the silicon etched in $TBABF_4$-only electrolytes is not hydrogen terminated, whereas the silicon is hydrogen terminated in the case of etching in HF-based electrolytes. The ability to complex silicon without HF or free fluorides provides a unique opportunity to etch silicon in the presence of a stable silicon dioxide layer and to evaluate alternatives to HF. In this work, we examine the voltammetry and oxidation-dissolution behavior of silicon using a variety of stable fluoride salts and examine the effect of surface oxides and water contamination.

Experimental

Prime grade n-type and p-type (100) silicon wafers were obtained from MEMC (Dallas, TX). The n-type silicon was doped with phosphorus and had a resistivity of 1-10 Ω cm. The p-type silicon was doped with boron and had resistivities of 1-10 Ω cm.

Acetonitrile was chosen as the solvent because of its high dielectric constant and electrochemical inertness. Anhydrous acetonitrile ($H_2O < 50$ ppm) was obtained from Aldrich Chemical (Milwaukee, WI). Further purification of the acetonitrile was accomplished by a series of vacuum distillation transfers followed by reflux over five chemical reagents[9] and by contact with activated alumina desiccant. The alumina desiccant, grade F-1, was purchased from Sigma Chemical (St. Louis, MO). The chemicals used in this study, $TBABF_4$, tetrabutylammonium hexafluorophosphate, tetrabutylammonium trifluoromethanesulfonate, sodium hexafluoroantimonate, boric acid, and potassium hexafluoroarsenate were obtained from Aldrich Chemical and dried under vacuum for at least 24 h prior to use. The materials were handled and experiments were performed in a Vacuum Atmospheres (Hawthorne, CA) inert atmosphere dry box maintained at less than 0.05 ppm water and 2 ppm oxygen. The electrochemical measurements were made using an EG&G Princeton Applied Research 273 (Princeton, NJ) potentiostat. A 0.65 mW HeNe laser with beam diameter of 0.47 mm was used in the photoetching studies. Neutral density filters were supplied by the Oriel Corporation (Stratford, CT).

The electrochemical experiments were carried out in a three-electrode Teflon reactor previously described.[9,10] Ohmic contacts were made to the back side of the wafer with gallium-indium alloy or by sputtering a 3000 Å aluminum layer. The reactor was filled in a dry box to protect it from atmospheric moisture and oxygen.

Results

Figure 1 shows the cyclic voltammogram of n-type silicon in 0.5 M $TBABF_4$/MeCN in the dark and illuminated. The onset of anodic photocurrent at n-type electrodes, which often correlates with the

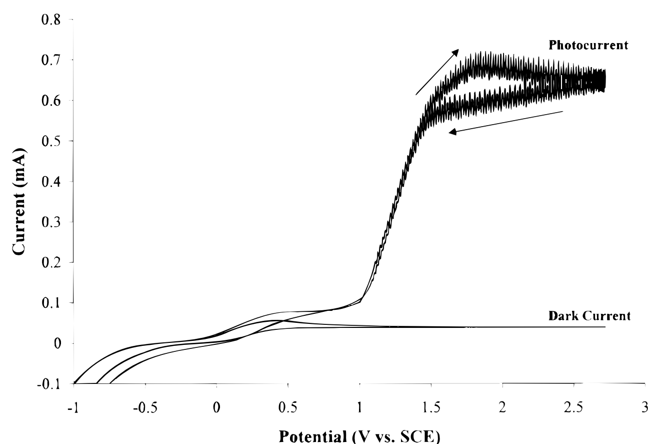

Figure 1. The photoelectrochemical behavior of n-type silicon in 0.5 M $TBABF_4$ in acetonitrile in the dark and under illumination. A 0.65 mW HeNe laser light source was used.

* Electrochemical Society Active Member.
** Electrochemical Society Student Member

S0013-4651(99)03-102-X CCC: $7.00 © The Electrochemical Society, Inc.

flatband potential (E_{FB}), was observed at potentials positive of −0.3 V *vs.* SCE on the positive-going scan. The photocurrents were relatively small in magnitude at potentials between −0.3 and 1.0 V on the first scan. The photoanodic current is due to the oxidation of silicon. Dissolution of the oxidized products occurs through formation of the fluoride complex. The oxidized silicon is able to extract fluoride ions from fluoroborate, leaving boron trifluoride products.[8] The quantum efficiency (number of electrons observed in the external circuit per absorbed photon) in this potential region was less than one. As the voltage was increased to values beyond 1.0 V *vs.* SCE, the photocurrent significantly increased. At potentials greater than 1.8 V, a photocurrent plateau was approximately 0.7 mA. This current corresponds to a quantum efficiency of approximately three. That is, photocurrent multiplication takes place and the value is lower than that observed for n-type silicon in HF in MeCN, which was about four.[8] The effect of protons is discussed in the next section.

The contribution of free-fluoride (*e.g.*, impurities from fluoroborate) on the anodic current was considered. The purity of the lithium fluoroborate as received was 99.999%, indicating that the starting materials were sufficiently pure. Boric acid was added to the electrolyte in one set of experiments. Boric acid will complex with free-fluoride generated during the experiments, producing fluoroborate. No differences in the current-voltage curves or silicon removal rate were observed. Finally, silicon dioxide was soaked in the fluoroborate electrolyte (as reported previously) and no dissolution of the oxide occurred.[8] Thus, it was concluded that trace impurities of free-fluoride did not have a significant impact on the observed behavior of silicon in the fluoroborate electrolytes.

The cyclic voltammogram of n-type silicon in 0.5 M $TBAPF_6$ in MeCN, shown in Fig. 2, is similar to that of n-type silicon in $TBABF_4$ in MeCN. Both electrolytes show small anodic photocurrents beginning at potentials positive of −0.3 V, and a large increase in photocurrent occurs at approximately 1.5 V *vs.* SCE. The quantum efficiency of n-type silicon in $TBAPF_6$, in MeCN is also approximately three electrons per incident photon and negligible anodic dark currents were observed. The photocurrent reached a plateau of 0.7 mA at approximately 2.2 V *vs.* SCE. The mass of silicon removed was compared to the total charge measured during the photoetching of a pit in the surface of the n-type silicon. 4 equiv/mol Si were measured, showing that tetravalent dissolution occurs in the electrolytes containing $TBABF_4$ and $TBAPF_6$ (Fig. 1 and 2).

Figure 3a shows the current-voltage curve for illuminated n-type silicon in 0.2 M $NaSbF_6$/MeCN. Etching was not observed in the dark even at high positive potentials. On the initial potential scan from −1 to 3 V *vs.* SCE under 0.65 mW HeNe laser illumination, only small photocurrents were observed, giving a quantum efficiency much less than one. The illuminated surfaces were not etched, as determined by visual inspection using an optical microscope. However, a slight roughening of the silicon surface occurred. The photocurrent could be due to silicon oxidation and reaction with traces of water in the solution. As the potential was scanned positive of 4 V (scan 1 of Fig. 3a), a significant increase in photocurrent was observed. Once the photocurrent and etching were initiated at high potentials, a photocurrent plateau was observed. The hysteresis between the forward scan (scan 1) and the reverse scan (scan 2) corresponds to a change in the electrode surface, most likely due to "breaking through" the surface oxide. As seen in Fig. 3a, the hysteresis is absent in the second positive-going scan (scan 3) and reversal (scan 4). In subsequent voltage cycles, scans 3 and 4 of Fig. 3a

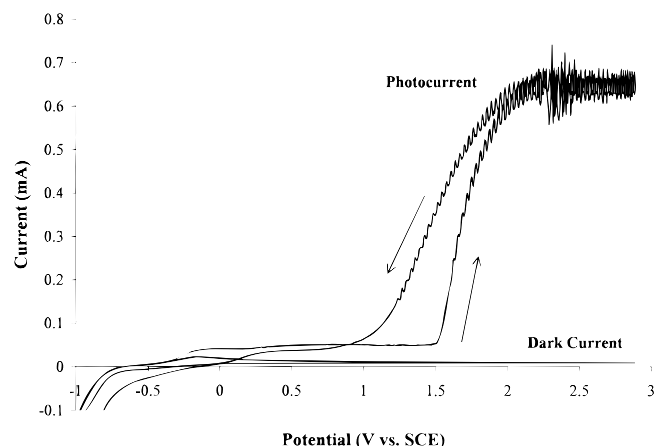

Figure 2. The photoelectrochemical behavior of n-type silicon in 0.5 M $TBAPF_6$ in acetonitrile in the dark and under illumination. A 0.65 mW HeNe laser light source was used.

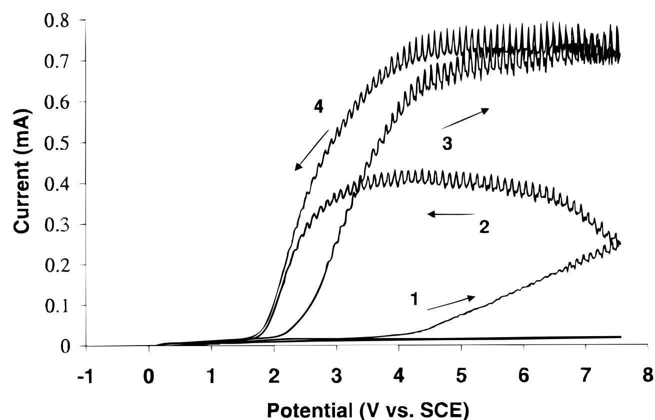

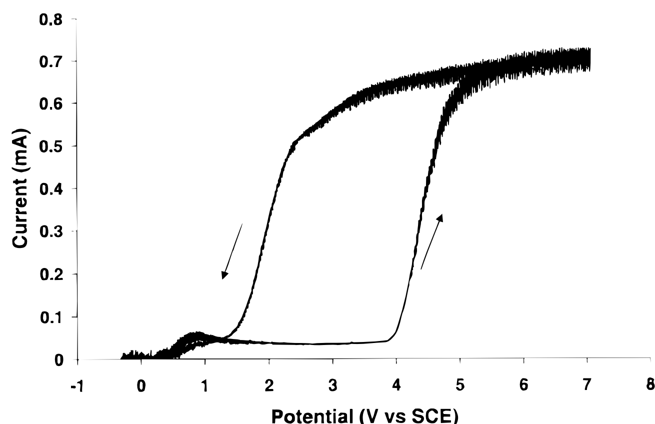

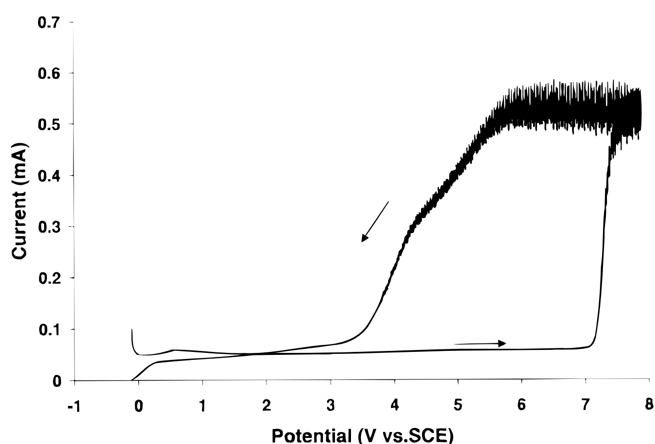

Figure 3. The photoelectrochemical behavior of n-type silicon (HeNe laser illumination) in (a, top) 0.2 M $NaSbF_6$ in acetonitrile, (b, middle) 0.2 M $KAsF_6$ in acetonitrile, and (c, bottom) 0.5 M $TBACF_3SO_3$ in acetonitrile.

S0013-4651(99)03-102-X CCC: $7.00 © The Electrochemical Society, Inc.

were replicated. The current-voltage curve showed negligible hysteresis and the onset potential remained at 1.75 V *vs*. SCE with a quantum efficiency of three. The quantity of silicon removed was compared to the charge passed during the experiment. The equivalents per mole values were determined from the amount of charge passed and the amount of silicon removed from the electrode. It was found that 11 equiv of charge were passed per mole of silicon removed using the 0.2 M $NaSbF_6$ in MeCN solution. This is different from the previous electrolytes where tetravalent dissolution was confirmed. It shows that other side reactions took place during the experiment. A similar hysteresis in the voltammogram was observed for n-type silicon in the 0.5 M $KAsF_6$/MeCN electrolyte (Fig. 3b). In this electrolyte, the onset potential in the forward scan occurred at approximately 4 V *vs*. SCE due to the presence of a native oxide. At potentials greater than 5 V, a photocurrent plateau of approximately 0.7 mA was observed, giving an apparent quantum efficiency of three. On the reverse scan, the onset potential was observed near 1.3 V *vs*. SCE. The equivalents per mole of silicon etched was found to be 14, showing that other reactions occurred during oxidation of the silicon. The current-voltage scan in 0.5 M $TBACF_3SO_3$/MeCN is shown in Fig. 3c. Although similar hysteresis and photocurrents were observed for n-type silicon in $TBACF_3SO_3$/MeCN, the photocurrent onset potential was more positive on both forward and reverse scans. The onset potential on the forward scan was at approximately 7 V *vs*. SCE. The magnitude of the current plateau was 0.5 mA, corresponding to an apparent quantum efficiency of 2.5. On the reverse scan, the photocurrent began to decrease at approximately 5.5 V and the onset potential was observed at approximately 2 V *vs*. SCE. It is not clear why the onset potential was more positive in the case of the $TBACF_3SO_3$ in MeCN as compared to the salts discussed previously. Changes in the equilibrium constant for the dissociation of the fluoride from the $CF_3SO_3^-$ complex may effect the onset potential. If the oxidized silicon intermediate is not able to strip fluoride from the $CF_3SO_3^-$ complex, then the silicon may have to be oxidized to a higher valence state before the fluorination. This could affect the potential (onset voltage) and quantum efficiency (photocurrent). Also, greater than seven electrons per silicon removed was measured.

The current-voltage behavior with $NaSbF_6$, $KAsF_6$, and $TBACF_3SO_3$ suggests that the etching is inhibited on the initial scan due the presence of a silicon dioxide layer formed prior to the electrochemical experiments. To investigate the effect of surface coverage of silicon dioxide, cyclic voltammetry of n-type silicon with native oxides and thermally grown oxides in the $TBABF_4$/MeCN and $TBAPF_6$/MeCN solutions was performed. Figure 4 shows the cyclic voltammogram for n-type silicon in 0.5 M $TBAPF_6$/MeCN with a 35 Å native oxide on the surface. The 35 Å oxide was measured by ellipsometry. In the experiment, the potential was scanned from −1 to 8 V *vs*. SCE. At approximately 7 V, the photocurrent increased, reaching a plateau of 0.65 mA. After scan reversal, a hysteresis was observed and the photocurrent onset was at more negative voltages, similar to Fig. 1 and 2. This current-voltage behavior, with a native oxide present, is nearly the same as those for n-type silicon in $TBACF_3SO_3$, $KAsF_6$, and $NaSbF_6$ (Fig. 3) electrolytes without an intentionally oxidized surface.

Silicon samples prepared with thin layers of thermally grown oxide (60 and 180 Å) were etched using the BF_4^- solutions. In order to etch the samples with 60 and 180 Å of thermally grown oxide, it was necessary to bias the silicon at 10 V *vs*. SCE for several seconds. The photocurrent observed from the silicon with the 60 and 180 Å oxide film was very large, like that in Fig. 2 or 3, and oscillated. The magnitude of the oscillations increased as the voltage increased. After the thermally oxidized silicon was illuminated and biased at 10 V *vs*. SCE for 30 s, the cyclic voltammogram was similar to that of silicon with no oxide present. High positive potentials were needed to remove the thin layers of oxide. Once the oxide was removed, the voltammetry was the same as in the absence of oxides.

The dependence of the photocurrent on light intensity was investigated using a series of neutral density filters. Cyclic voltammograms for n-type silicon in 0.5 M $TBABF_4$/MeCN using a 0.65 mW HeNe laser and a variety of neutral density filters are shown in Fig. 5. The water contamination in this electrolyte was found to be approximately 30 ppm by Karl Fischer analysis. The incident light power was varied from 1 to 100% of full laser power (0.65 mW). As the light intensity increased, the photocurrent plateau increased linearly and current oscillations were observed. At 10 and 16% of the full laser power, the photocurrent was constant with time (no oscillations). At higher incident powers (*i.e.*, >20%), oscillations were observed at potentials positive of 1.8 V *vs*. SCE. At 26.5% of full laser power, oscillations were observed at all potentials on the photocurrent plateau. At low light intensities and low anodic potentials, the rate of oxide formation (due to residual water) is lower and the oxides are less dense and more nonuniform. At higher light intensities, more uniform oxides with a higher density may be present. The onset of oscillations at higher potentials and higher intensities indicates that the oscillations are associated with a higher rate of oxide formation and periodic dielectric breakdown.

The current oscillations during silicon etching in fluoride-free, nonaqueous solutions were found to be dependent on the water concentration. The current-voltage behavior of silicon in $TBABF_4$/MeCN as a function of water concentration is shown in Fig. 6. There were no changes in onset potential or plateau current when

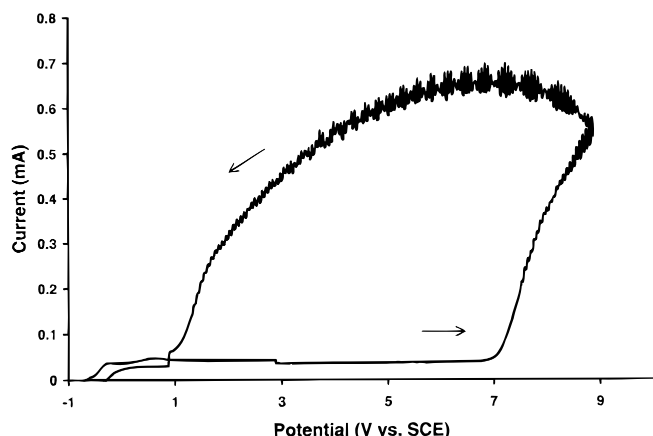

Figure 4. The photoelectrochemical behavior of n-type silicon with a thin surface oxide in 0.5 M $TBAPF_6$ in acetonitrile in the dark and under illumination. A 0.65 mW HeNe laser light source was used.

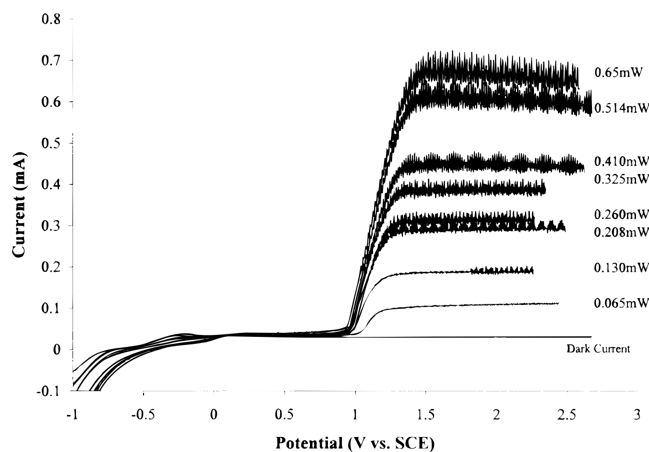

Figure 5. Cyclic voltammogram for illuminated n-type silicon in 0.5 M $TBAPF_6$ in acetonitrile at different light intensities. Neutral density filters were used to vary the light intensity of the HeNe laser light source. The power of the light source and the neutral density filter is listed next to the photocurrent curve.

S0013-4651(99)03-102-X CCC: $7.00 © The Electrochemical Society, Inc.

the water concentration was increased from 15 to 40 ppm. Each voltammogram (Fig. 6a and b) exhibited a photocurrent onset potential at approximately −0.5 to 0 V *vs*. SCE and the highest photocurrent occurred in the potential region of 1.5 to 3 V *vs*. SCE . The addition of water increased the magnitude of the photocurrent oscillations. Notable effects also appeared when comparing the equivalents per mole of silicon etched. When the water concentration was less than 15 ppm, approximately 4 equiv/mol were measured. As the water concentration increased to values greater than 50 ppm, approximately 32 equiv/mol were measured. Values greater than four indicate side reactions have occurred that do not result in silicon etching. The current may be due to electrochemical production of silicon dioxide and/or solvent oxidation.

Discussion

The electrochemical oxidation and dissolution of silicon involves a series of electron-transfer and chemical steps beginning with silicon starting in the zero-valent form and ending in the tetravalent hexafluoride complex. The sequence is initiated by valence band holes and involves intermediates that have (*i*) electrons in high energy levels allowing electron injection into the conduction band and (*ii*) a strong affinity for fluoride ions. The affinity for fluoride ions is evident by the sustained oxidation and dissolution of silicon in the absence of hydrogen fluoride and water, as demonstrated here in MeCN. Although the equilibrium of the BF_4^- fluoride complex and other complexes (*e.g.*, PF_6^-, $CF_3SO_3^-$, AsF_6^-, and SbF_6^-) fails to yield an appreciable concentration of free-fluoride, each of the fluoride-containing complexes is susceptible to fluoride scavenging. The partially oxidized silicon on the electrode surface has a high affinity for fluoride, which can be obtained for the salt used. For example, the dissociation of fluoroborate is shown in Eq. 1 [11]

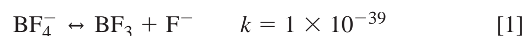

$$BF_4^- \leftrightarrow BF_3 + F^- \qquad k = 1 \times 10^{-39} \qquad [1]$$

The ability of silicon to electrochemically dissolve in the presence of these salts (without HF or free fluoride) demonstrates the relative strength of the silicon-fluoride complex. In aqueous electrolytes, no dissolution of silicon occurs in the presence of these salts (without HF).

The current-voltage behavior of silicon in $TBABF_4$/MeCN and $TBAPF_6$/MeCN are remarkably similar and exhibit minimal current-voltage hysteresis or surface passivation. The onset potentials observed when silicon is anodized in either $TBABF_4$ or $TBAPF_6$ were shifted to more positive potentials compared to the anhydrous HF in MeCN electrolyte. Previous results have shown that the silicon-hydride surface formed during etching in HF/MeCN is absent when etching in $TBABF_4$/MeCN.[8] The loss of surface bound hydrogen can result in an increase in the surface state density on the silicon electrode. The onset potential (*i.e.*, flatband potential) is also affected by the presence of charged species surface states. The Fermi level would shift to more positive potentials, if the surface were more positively charged compared to the hydride-terminated surface. It is interesting to note that a small photocurrent is observed in Fig. 1 and 2 at the same onset potential as observed with HF in the electrolyte.

The electrochemical passivation of n-type silicon in $TBACF_3SO_3$, $KAsF_6$, and $NaSbF_6$ in MeCN, as seen in the current-voltage behavior, appears to be related to the higher water contamination in these electrolytes (>50 ppm) and lower fluoride dissociation constants. The potential for the onset of photocurrent in these electrolytes was similar to the onset potential observed in $TBAPF_6$/MeCN, when a native oxide was present, showing the presence of an oxide blocking layer. This thin oxide was most likely formed by the reaction of silicon with traces of water in the electrolyte. Without HF, silicon dioxide does not dissolve. Removal occurs here via dielectric breakdown, ion transport, and oxidation of the underlying silicon. Following breakdown of the oxide, the silicon is exposed and oxidation can progress, possibly through pits or defects in the low-quality oxide. Additional chemical analysis of the solutions and the etched silicon is needed to determine the nature of the surface passivation in the alternate fluoride salt solutions.

The presence of oxides resulting from water contamination leads to the creation of photocurrent oscillations. The buildup and breakdown of the oxide layer has been studied in aqueous electrolytes by several authors.[3-6] The oscillation models developed from results in aqueous solutions do not fully explain the oscillation behavior in nonaqueous, fluoride-free electrolytes. In these nonaqueous solvents, there is no chemical dissolution of the silicon dioxide. Previous results have shown that there was no measurable etch rate for silicon dioxide dissolution in MeCN solutions containing $TBABF_4$. The oscillation models of Gerischer and Lubke[3] and Chazalviel *et al*.[4] represent the structure of the oxide divided into two homogeneous films: a dense oxide film with low defect levels and a less-dense film with high defect concentration. The ionic transport through the oxide films resulted in dissolution and control of the current oscillations. The oscillation mechanisms presented by Lehman[6] and Carstensen *et al*.[5] also included ion transport in the oxide layer, and localized failures occur by either physical failure of the oxide or by ionic breakthrough which creates channels or pores. In each of the aqueous models, the dissolution of the oxide by the fluoride-containing electrolyte was an essential and contributing factor to the oscillations. However, in those studies it was not possible to evaluate the oscillation behavior in the absence of SiO_2 dissolution because the HF (or other fluorides) was needed to maintain etching in the aqueous electrolytes. Thus, this is the first opportunity to observe oscillations during the oxidation and dissolution of silicon without the dissolution of SiO_2. Thus, it is clear that SiO_2 chemical dissolution is not an essential component to obtain oscillations.

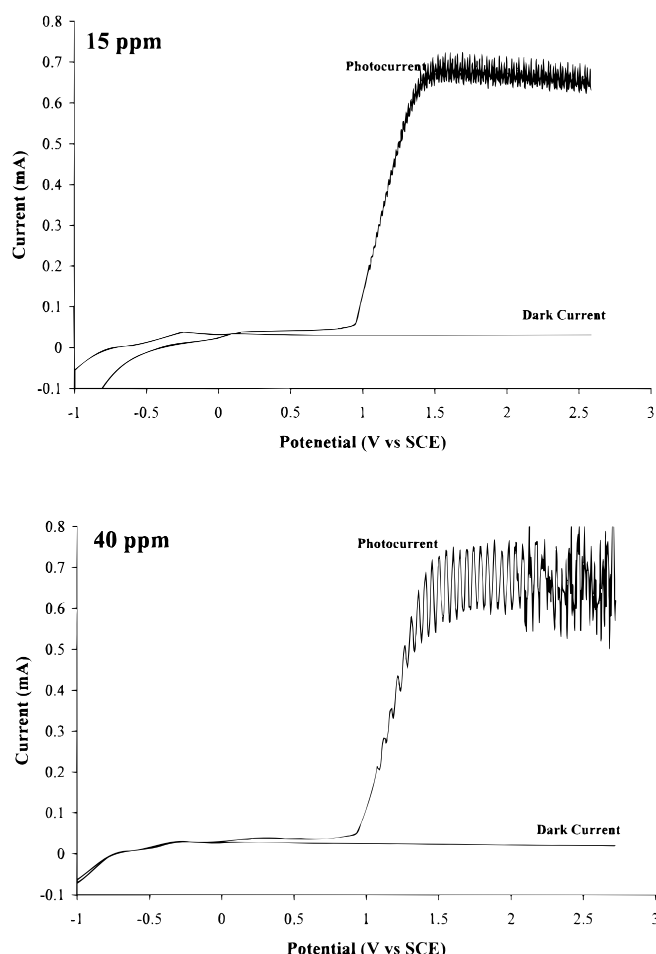

Figure 6. The current-voltage behavior of n-type silicon in 0.5 M $TBABF_4$ in acetonitrile in the dark and under illumination at (a, top) 15 ppm water concentration and (b, bottom) 40 ppm water concentration.

S0013-4651(99)03-102-X CCC: $7.00 © The Electrochemical Society, Inc.

The oscillations observed here are different in several respects compared to aqueous conditions. First, the etching and oxidation does not occur across the entire surface since the electrode was illuminated with a 0.47 mm diam laser beam. Second, the frequency of the oscillations is higher than those observed in aqueous electrolytes. Oxide growth arises from the trace water in solution and the reactivity of the silicon with water. The effect of increasing the water concentration is clearly seen in Fig. 6, where the increased water concentration caused an increase in the frequency and intensity of the current oscillations. Because the chemical dissolution of oxide is not possible in the nonaqueous, non-HF electrolytes, the current oscillations must be related to the formation of the oxide layers from residual water and subsequent oxide breakdown at high anodic bias. The current oscillations illustrate the complications caused by water on the silicon reactions at low water concentrations.

The substitution of a fluoride complex for hydrogen fluoride in the nonaqueous etching of silicon changes the apparent quantum efficiency. The anodization of silicon in MeCN without free-fluoride resulted in quantum efficiencies of two to three, whereas values of three to four were obtained in anhydrous HF in MeCN. Previous n-type silicon mid-infrared Fourier transform infrared (MIR-FTIR) studies of silicon etching in BF_4^- in MeCN have shown that BF_3 is produced by stripping a fluoride from the BF_4^-.[8] In the presence of HF (*i.e*., the availability of protons), a hydride-terminated surface is created due to the addition of HF across Si-Si back bonds.[8] The absence of protons in the case of BF_4^-, PF_6^-, $CF_3SO_3^-$, AsF_6^-, and SbF_6^- forces the final Si-Si bond to undergo electrochemical oxidation, leaving the surface in a nonhydride termination state. This electrochemical route does not contribute to the current multiplication, thus lowering the overall quantum efficiency. The presence of surface states may also contribute to the decrease in overall quantum efficiency, since these calculations did not include the effect of recombination at the nonhydride surface.

Conclusions

In this study we have demonstrated that silicon can be oxidized and dissolved in acetonitrile solutions by use of anions such as BF_4^-, PF_6^-, $CF_3SO_3^-$, AsF_6^-, or SbF_6^- in place of free-fluoride. The current-voltage behavior of n-Si in these electrolytes was not the same as in electrolytes containing HF, indicating an alternate oxidation-dissolution pathway. Furthermore, we have demonstrated the ability to initiate and sustain etching of silicon-containing surface oxides where the oxide is not soluble in the electrolyte. Photocurrent oscillations have been observed in electrolytes without HF or free-fluoride present. The ability to complex silicon using alternate fluoride sources demonstrates the possibility of designing either chemical or electrochemical methods for the oxidation and dissolution of silicon in the absence of free-fluoride where silicon dioxide is stable (not soluble).

The Georgia Institute of Technology assisted in meeting the publication costs of this article.

References

1. P. Allongue, V. Kieling, and H. Gerischer, *Electrochim. Acta*, **40**, 1353 (1995).
2. C. Levy-Clement, A. Lagoubi, R. Tenne, and M. Neumann-Spallart, *Electrochim. Acta*, **37**, 877 (1992).
3. H. Gerischer and M. Lubke, *Ber. Bunsen-Ges. Phys. Chem*., **92**, 573 (1988).
4. J.-N. Chazalviel, C. da Fonseca, and F. Ozanam, *J. Electrochem Soc*., **145**, 964 (1998).
5. J. Carstensen, R. Prange, G. S. Popkirov, and H. Foell, *Appl. Phys. A*, **67**, 459 (1998).
6. V. Lehman, *J. Electrochem Soc.*, **143**, 1313 (1996).
7. H. Kikuyama, M. Waki, M. Miyashita, T. Yabune, N. Miki, J. Takano, and T. Ohmi, *J. Electrochem Soc.*, **141**, 366 (1994).
8. J. C. Flake, M. M. Rieger, G. M. Schmid, and P. A. Kohl, *J. Electrochem Soc*., **146**, 1960 (1999).
9. E. Propst and P. A. Kohl, *J. Electrochem. Soc*., **140**, L78 (1993).
10. M. M. Rieger and P. A. Kohl, *J. Electrochem. Soc*., **142**, 1490 (1995).
11. *Advances in Fluorine Chemistry*, M. Stacey, J. C. Tatlow, and A. G. Sharpe, Editors, Vol. 1, p. 72, Academic Press, New York (1960).